

Interferometric Down-Conversion of High-Frequency Molecular Vibrations with Time–Frequency-Resolved Coherent Raman Scattering Using Quasi-CW Noisy Light: C–H Stretching Modes of Chloroform and Benzene

Darin J. Ulness, Michael J. Stimson, Jason C. Kirkwood, and A. C. Albrecht*

Department of Chemistry, Baker Laboratory, Cornell University, Ithaca, New York 14853

Received: March 6, 1997; In Final Form: April 22, 1997[⊗]

For the first time, the high-frequency symmetric C–H stretching modes of chloroform and benzene are down-converted using the recently developed time–frequency-resolved interferometric coherent anti-Stokes Raman scattering with broad-band nontransform limited (noisy) light excitation method. As an application, chloroform–carbon tetrachloride, benzene–benzene- d_6 and benzene–acetone- d_6 dilution series are performed. Concentration-dependent Raman frequencies and vibrational dephasing rate constants are observed by this new technique.

I. Introduction

Vibrational dynamics in liquids have been of great interest for many years. Two parameters are of prime concern in the short time domain; the vibrational frequency, ω_R , and (in the fast modulation limit for the line-shaping stochastic process) the vibrational dephasing rate constant γ_R . By the 1970's, the wide availability of lasers had advanced understanding of the underlying mechanisms of vibrational dynamics in liquids,¹ and to date a considerable amount of theoretical and experimental literature exists on the subject—a comprehensive collection of references may be found in a recent review.²

In this article, we are concerned with the vibrational dynamics (ω_R and γ_R) of the symmetric C–H stretch³ ($\tilde{\nu}_R$), observed by an entirely new experimental method. Using interferometric coherent Raman scattering (CRS) based on noisy light, data are presented for C–H stretching motions in chloroform and benzene at various dilutions. The C–H stretch is of much importance, for a number of reasons. It is a high-amplitude “external” mode whose dynamic properties can be especially sensitive to its condensed phase environment. Furthermore, the C–H modes are relatively isolated from the remainder of the intramolecular vibrational space and therefore can often be considered “pure.” The C–H stretches of chloroform and benzene have been studied with regard to effects due to added diluents^{4–11} and sensitivity to changes in temperature^{12–14} and pressure.^{15,16} They thus provide a good context for examining this new experimental method.

The most common experimental approaches to the probing of vibrational dynamics in liquids are steady state IR and Raman spectroscopies and time-resolved Raman techniques (impulsive Raman, picosecond and femtosecond time resolved coherent Raman scattering (TR-CRS), etc.) The technique presented in this work involves the use of broad-band quasi-CW (nontransform-limited) noisy light interferometrically in CRS spectroscopy. The method can be considered as one that is intermediate in nature between steady state spectroscopy and the pure time resolved techniques.

In the early 1980's, it was shown that noisy light offers a time resolution on the order of the noise correlation time, τ_c , of the light (typically tens to several hundreds of femtoseconds)—many orders of magnitude faster than the temporal profile of the light (often several nanoseconds, but in principle CW).¹⁷ A

critical review of many applications of noisy light is given by Kobayashi.¹⁸ A more recent review by Kummrow and Lau¹⁹ contains an extensive listing of references.

A typical noisy light experiment involves the splitting of a noisy beam into identical twin beams, B and B', through the use of a Michelson interferometer. One arm of the interferometer is computer controlled to introduce a relative delay, τ , between B and B'. The twin beams exit the interferometer and are focused into a sample. Additional beams (either broad-band or narrow-band) may also be focused into the sample in accordance with the desired experimental beam geometry and the nonlinear spectroscopy of choice. The delay between B and B' is then scanned and the frequency-resolved signal intensity of interest is detected as a function of τ to produce an *interferogram*. The particular noisy light experiment used in this paper is based on coherent anti-Stokes Raman scattering (CARS) in which the actions of B and B' are joined by an action of a narrow-band field, M, to produce (speaking perturbatively) the CARS-type third-order polarization. As an interferometric spectroscopy, it has come to be called I⁽²⁾CARS.^{20,21} It is based on the theory of “monochromatically” detected I⁽²⁾CARS developed by Dugan et al.^{22–24} and expanded upon by Schaertel et al.^{25,26} The theory predicts that the so-called radiation difference oscillations²⁷ (RDOs) should appear in the “monochromatically” detected I⁽²⁾CARS interferogram with a frequency $\Delta \equiv \omega_M + 2\omega_R - \omega_D$, where ω_D is the detected frequency, ω_M is the narrow-band frequency, and ω_R is the Raman (vibrational) frequency. Since ω_D and ω_M are known, ω_R may be extracted from the experimentally measured RDOs. Furthermore, the dephasing rate constant, γ_R , is determined from the observed decay rate constant, γ , of the I⁽²⁾CARS interferogram. For the I⁽²⁾CARS signal, whenever $\omega_D \approx \omega_M + 2\omega_R$ we have $\Delta \approx 0$. That is, the RDOs are strongly down-converted representations of the Raman frequency. This down-conversion is one of the chief advantages of the I⁽²⁾CARS technique, because it allows for the characterization of vibrations with a much smaller sampling rate than would be required if the modes were not down-converted. More explicitly, the Nyquist sampling rate criterion for the RDOs is much smaller than that for the vibration itself. This is particularly true for high-energy modes such as the C–H vibrations studied here.

We present here, for the first time, the down-conversion of the high frequency C–H stretching mode using the newly developed frequency-resolved I⁽²⁾CARS method.²⁸ Very re-

[⊗] Abstract published in *Advance ACS Abstracts*, June 1, 1997.

cently, the I⁽²⁾CARS method has been extended to a two-dimensional time–frequency technique in which the entire I⁽²⁾CARS signal spectrum is detected (via chromatic dispersion onto a charge coupled device (CCD) array) for each delay setting (τ). In principle, no additional information is gained by simultaneously detecting more than a single frequency; in practice, however, this extension provides a nearly three orders of magnitude redundancy in the data. The quality of the extracted spectroscopic and dynamic parameters, namely ω_R and γ_R , is greatly improved without additional acquisition time. The time–frequency data sets are referred to as *spectrograms*.

The advantages of I⁽²⁾CRS spectrograms are best seen when the Raman cross-section is strong and the dephasing is slow—corresponding to an intense narrow line in the conventional spontaneous Raman spectrum. The I⁽²⁾CARS spectrogram of the “ring breathing” mode of benzene provides an excellent example.²⁹ The main focus of the present work is to apply I⁽²⁾-CARS to down-convert C–H stretching modes—an important class of vibrations. Though this class of vibrations tends to dephase rapidly, we shall see that I⁽²⁾CARS spectrograms can be recorded and useful information obtained from them.

The I⁽²⁾CARS signal (at the intensity level) can be viewed as the sum of three contributions: (i) a purely resonant contribution, (ii) a purely nonresonant contribution, and (iii) a resonant–nonresonant cross term contribution. At the polarization (amplitude) level there is a resonant term stemming from the Liouville paths³⁰ that contain a Raman resonance after the second field intervention in the perturbative development of the third-order polarization. Conversely, a nonresonant term arises from all Liouville paths that do not contain a resonance. Since the I⁽²⁾CARS signal is detected at the intensity (mod-square) level, one clearly obtains the two pure terms (i and ii) along with the cross term (iii). Theory^{23,25,26} shows that for a conventional Bloch two-level system an excellent approximation³¹ to the I⁽²⁾CARS signal is given by

$$I(\tau, \omega_D) \approx K(\omega_D) e^{-2\gamma|\tau|} \frac{\cos \Delta\tau}{2\gamma} + 2RK(\omega_D) e^{-2\gamma|\tau|} \frac{\sin \Delta|\tau|}{\gamma} + 2R^2K'(\omega_D) e^{-2\Gamma|\tau|} + \text{background} \quad (1)$$

where $K(\omega_D)$ and $K'(\omega_D)$ are the resonant and nonresonant I⁽²⁾-CARS spectra respectively, $\gamma = \gamma_R + \gamma_D/2 + \gamma_M/2$ where γ_D and γ_M are the half-widths of the monochromator slit function and the narrow-band beam, respectively—both are much smaller than γ_R in these studies. R is the ratio of the nonresonant to resonant hyperpolarizability²⁵ and $\Gamma \approx 1/\tau_c$. The background term is τ -independent and is not used to extract dynamical information. In this paper $K(\omega_D)$ and $K'(\omega_D)$ are empirical functions, though for the theoretical model^{20,22} they are explicit functions.

It is straightforward but tedious to extend (1) to the case of mixtures. For the special case of a binary mixture (A with mole fraction X_A and B with mole fraction X_B) where species A is potentially vibrationally resonant, but species B is never resonant, (1) becomes^{25,26}

$$I(\tau, \omega_D) \approx X_A^2 K(\omega_D) e^{-2\gamma|\tau|} \frac{\cos \Delta\tau}{2\gamma} + 2X_A^2 R_A K(\omega_D) \times e^{-2\gamma|\tau|} \frac{\sin \Delta|\tau|}{\gamma} + 2X_A X_B R_B K(\omega_D) e^{-2\gamma|\tau|} \frac{\sin \Delta|\tau|}{\gamma} + [2X_A^2 R_A^2 + 4X_A X_B R_A R_B + 2X_B^2 R_B^2] K'(\omega_D) e^{-2\Gamma|\tau|} + \text{background} \quad (2)$$

where R_A and R_B are the ratios of the nonresonant hyperpolarizabilities of A and B, respectively, to the resonant hyperpo-

larizability of species A. Now we have two types of cross terms: those of resonant A–nonresonant A (second term in (2)) and resonant A–nonresonant B (third term in (2)). Since the material dephasing dynamics is contained in the γ decay, which is much slower than the autocorrelation decay of the noisy light (the Γ decay), we simply exclude early delay times, $|\tau| < 200$ fs (the coherence spike) and fit any given I⁽²⁾CARS spectrogram to the equation,

$$I(\tau, \omega_D) \approx K(\omega_D) \left\{ e^{-2\gamma|\tau|} \frac{\cos \Delta\tau}{2\gamma} + 2 \left[R_A + \left(\frac{X_A}{X_B} \right) R_B \right] e^{-2\gamma|\tau|} \frac{\sin \Delta|\tau|}{\gamma} \right\} + \text{background} \quad (3)$$

to extract ω_R (via the Δ s), γ_R (via γ), and the quantity $[R_A + (X_A/X_B)R_B]$.

In summary, time–frequency-resolved I⁽²⁾CARS offers simultaneous multichannel detection (each pixel represents a single “monochromatically” detected I⁽²⁾CARS interferogram), which affords a very large data redundancy. The time-resolved dispersed I⁽²⁾CARS signal appears for any given pixel as an interferogram having RDOs representing the strongly down-converted Raman vibration. Furthermore, the resonant to nonresonant ratio of the hyperpolarizability is recovered. Independent knowledge of one hyperpolarizability of the ratio leads to the absolute measure of the other. Dilution studies can then be done to determine the nonresonant hyperpolarizability of the diluent. This last point will not be discussed further since the main focus of the paper is the down-conversion of the high frequency C–H modes, a class of vibrations not optimal for determining the diluent’s nonresonant hyperpolarizability. (Use of any strong, sharp, Raman resonance, such as the “ring breathing” mode of benzene,²⁹ for this purpose is preferable.)

II. Experiment

The broad-band and narrow-band light sources are simultaneously pumped by a single Q-switched Nd:YAG laser (Spectra-Physics DCR 2A). The narrow-band source is a commercial dye laser (Spectra-Physics) operating at fifth-order diffraction (hwhm ≈ 0.2 cm⁻¹). The broad-band noisy light source is a home-built two-stage laser. The first stage is an oscillator which consists of a transversely pumped dye cell in a cavity having a high-reflectivity end mirror and a glass plate output coupler. This allows for much of the emission spectrum of the dye to exit the cavity. The light from the oscillator stage is amplified in the second stage which consists of a single longitudinally pumped dye cell.

For this experiment the narrow-band dye laser contained LDS 751 (Exiton) in methanol, and the noisy light source contained Sulforhodamine 640 (Exiton) in methanol. The bandwidth, Γ , of the noisy light is about 100 wavenumbers and has a correlation time of ~ 100 fs (half width at half-maximum, hwhm).

The noisy beam is passed through a Michelson interferometer where one arm is movable via a computer-controlled stepping motor delay line (Klinger). The narrow-band beam (M) joins the emergent twin noisy beams (B and B') in the BOX beam geometry³² which are then focused into the sample cell. The sample cell is a 1 cm flow cell which allows for easy sample changing with minimal perturbation of the system. The I⁽²⁾-CARS signal (propagating along its own unique k vector) is coarsely spatially filtered and sent through a SPEX 1 m double-grating monochromator with its middle and exit slits removed.

In this way an approximately 10 nm spectral window is dispersed onto 1024 pixels of a CCD array (EG&G). The ultimate resolution of the technique, however, was determined by measuring the widths of neon lines (0.225 cm^{-1} (hwhm)) used for absolute frequency calibration. The samples; chloroform and benzene (both from Fisher), and the diluting solvents, carbon tetrachloride (Fisher), benzene- d_6 , and acetone- d_6 (both from Isotope Laboratories), were all used without further purification. All experiments were carried out under an ambient temperature of $18 \text{ }^\circ\text{C}$.

III. Results and Discussion

Time–frequency $I^{(2)}$ CARS spectrograms were obtained for the (symmetric) C–H stretches in chloroform and benzene. The dilutions series: chloroform–carbon tetrachloride, benzene–benzene- d_6 , and benzene–acetone- d_6 were performed. The chloroform data were found to be more precise than the benzene data because chloroform produced a higher signal to noise ratio.

Figure 1a shows a spectrogram of the $I^{(2)}$ CARS signal for the symmetric C–H stretch of neat benzene. The narrow-band light (M) was set at roughly 744 nm (more precisely at $13\,440.0 \pm 0.5 \text{ cm}^{-1}$). The detection frequency window ($19450\text{--}19700 \text{ cm}^{-1}$) covers, in this case, 621 pixels (of a possible 1024) of the CCD array. Thus there are 621 “monochromatically” detected interferograms contained in one such spectrogram each corresponding to a different setting of ω_D . That is, each pixel samples the signal at a distinct ω_D . The detected frequency where the RDO vanishes ($\Delta = 0$) occurs at precisely $19\,564.0 \pm 0.5 \text{ cm}^{-1}$. To illustrate, the time axis of the spectrogram (Figure 1a) has been Fourier transformed to produce a RDO-frequency-detected frequency plot shown in Figure 1b. The pronounced line labeled “ Δ ” in Figure 1b gives Δ at each ω_D . $|\Delta/2\pi c|$ is seen to range from 0 to 300 cm^{-1} representing a dramatic down-conversion of the C–H stretching mode ($\sim 3000 \text{ cm}^{-1}$). The zero of Δ is found at the intersection of this line with the abscissa. The pronounced line labeled “ $-\Delta$ ” consists of the “negative” frequency components of the transformed RDOs.³³ This line is not removed since it aids the eye in estimating $\Delta = 0$.

Visually, the spectrogram in Figure 1a is symmetric in τ (as can be inferred from (2)), but there is a slight asymmetry about $\Delta = 0$ (the dark central peak appears to be skewed toward lower frequencies—toward positive Δ).³⁴ This is due to the resonant–nonresonant cross terms (terms 2 and 3) in (2) which are symmetric about $\tau = 0$ but asymmetric about $\Delta = 0$ through the term containing $\sin |\Delta|\tau|$. When Δ is positive, the contribution of the cross terms for small $|\tau|$ is also positive. Conversely, when Δ is negative, the initial contribution of the cross terms is also negative. A similar asymmetry is found in the chloroform C–H spectrograms (not shown). This means that the nonresonant contribution to the $I^{(2)}$ CARS signal is significant. This can be contrasted with the ring breathing (992 cm^{-1}) mode of benzene in which the resonant contribution completely dominates the hyperpolarizability,²² and the spectrograms for this mode show no visually noticeable asymmetry.²⁹

To extract the dynamic and spectroscopic parameters (γ_R and ω_R) from the spectrograms, (3) is used in a Levenberg–Marquardt based fitting routine. As stated, data for $|\tau| < 200$ fs are removed prior to fitting to eliminate the need to fit the coherence spike. Data at frequencies near $\Delta = 0$ are also removed before fitting to avoid any possible interference due to the presence of twice anti-Stokes shifted stimulated Raman scattering of the narrow-band beam. (This would appear precisely at the $\Delta = 0$ frequency.) The average fitting time is roughly 1 h per spectrogram when running on an 75 MHz Intel

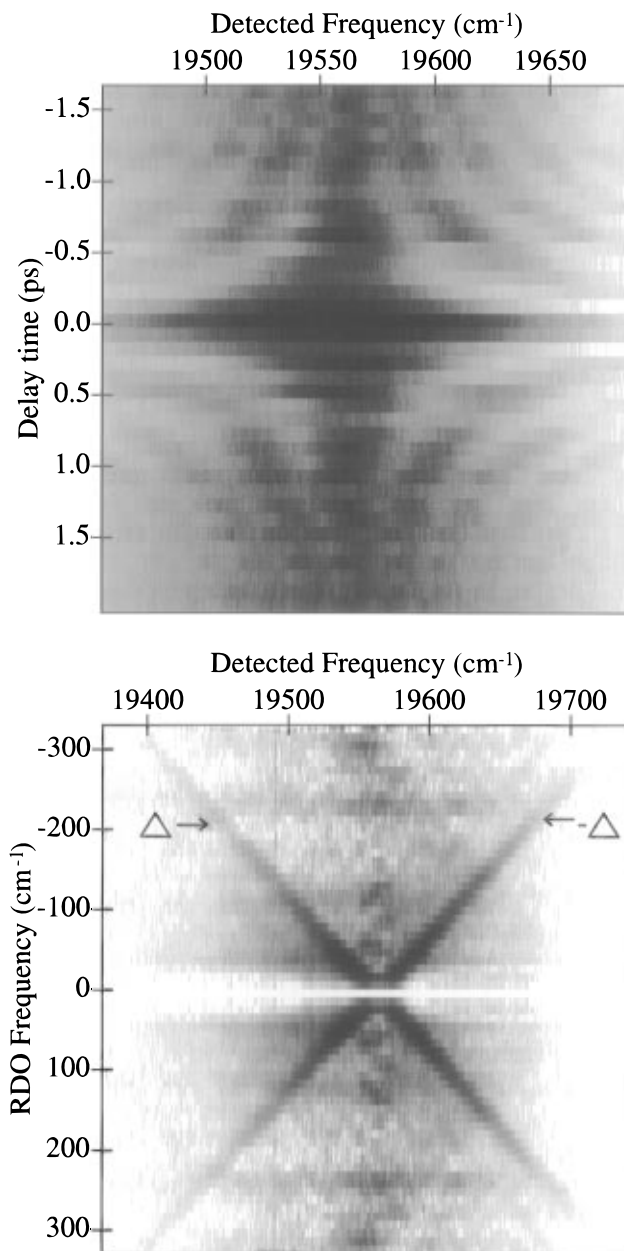


Figure 1. (a) The raw data from the frequency-resolved detection of the $I^{(2)}$ CARS signal from the symmetric C–H stretching mode of neat benzene displayed as a spectrogram. The darker regions indicate greater signal intensity. The narrow-band beam was tuned to $13440.0 \pm 0.5 \text{ cm}^{-1}$. The zero of Δ occurs for a detector setting of $19564.0 \pm 0.5 \text{ cm}^{-1}$ and appears as the dark vertical feature. The coherence spike at $\tau = 0$ appears as the dark horizontal feature. The central feature appears to be skewed toward positive Δ . This is a manifestation of the resonant–nonresonant cross terms (2) which are asymmetric in Δ . (b) The time-to-frequency Fourier transform of (a). The value of Δ for each value of ω_D (in units of wavenumbers) forms the dark feature labeled “ Δ ”. The feature labeled “ $-\Delta$ ” is the “negative” component of the recovered frequency³³ Δ which is kept simply for convenience and to aid the eye in estimating the position of $\Delta = 0$. The zero of Δ occurs at the intersection of the two diagonal features.

Pentium processor (the actual time depends on the initial parameters and the size of the data set).

Figure 2 reports $\tilde{\nu}_R$ ($\omega_R/2\pi c$) and γ_R (hwhm) for the C–H stretch of chloroform in a dilution series with carbon tetrachloride. The values of $\tilde{\nu}_R$ and γ_R for neat chloroform are $3018.24 \pm 0.31 \text{ cm}^{-1}$ and $1.03 \pm 0.07 \text{ ps}^{-1}$, respectively. The apparent vibrational frequency is seen to be gradually red-shifted upon going from neat chloroform ($X_{\text{HCCl}_3} = 1$) to roughly a mole fraction of 0.5 in carbon tetrachloride below which the red shift

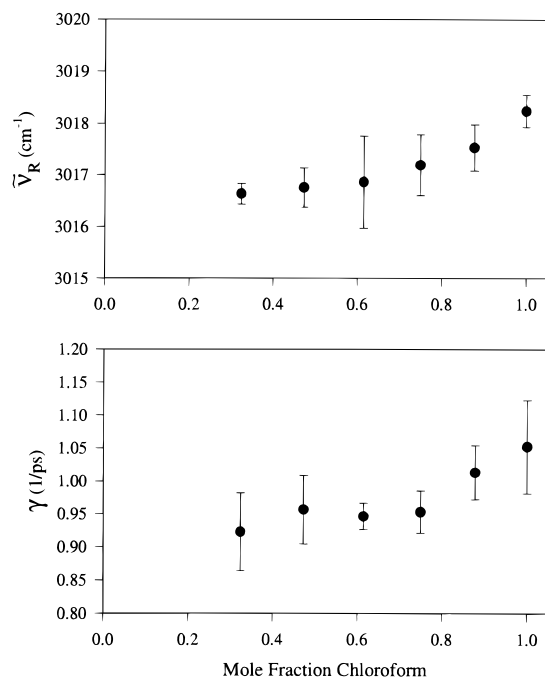


Figure 2. Recovered values of $\tilde{\nu}_R$ and γ for the dilution series of chloroform in carbon tetrachloride. The error bars indicate the standard deviation of four dilution series performed on two separate days. The average relative standard deviation for the chloroform data is 0.016%.

TABLE 1: Summary of Results Presented in This Work

	neat $\tilde{\nu}_R$ (cm^{-1})	$\Delta\tilde{\nu}_R^{(0.5)}$ (cm^{-1})	neat γ_R (ps^{-1})	$\Delta\gamma_R^{(0.5)}$ (ps^{-1})
chloroform—carbon tetrachloride	3018.24	1.67 (red shift)	1.03	0.10
benzene—benzene- d_6	3062.88	0.89 (blue shift)	0.85	slight increase
benzene—acetone- d_6	3062.88	1.87 (blue shift)	0.85	slight increase

begins to slow. For comparison with the literature (below) let $\Delta\tilde{\nu}_R^{(0.5)}$ define the observed vibrational frequency shift (relative to the neat solution) at 0.5 mole fraction. We find for chloroform in carbon tetrachloride $\Delta\tilde{\nu}_R^{(0.5)} = 1.67 \text{ cm}^{-1}$. The apparent dephasing rate constant, γ_R , is seen to decrease upon dilution with $\Delta\gamma_R^{(0.5)} = 0.10 \text{ ps}^{-1}$. The average of the relative standard deviation for the $\tilde{\nu}_R$ measurements is 0.016% (or $\pm 0.56 \text{ cm}^{-1}$ for this C—H mode), and for the γ_R measurements it is 4.8%. The extracted value of the quantity $[R_A + (X_A/X_B)R_B]$ (from (3)) is not very precise for this particular system. Nonetheless, R_A for neat chloroform is found to be 0.465 ± 0.09 . But because of the imprecision of the recovered values of $[R_A + (X_A/X_B)R_B]$ and the loss of signal at small mole fractions of chloroform, R_B could not be extracted reliably. As mentioned, other Raman transitions can provide much more precise values of R_A and R_B .²⁹ The results are summarized in Table 1.

Figure 3 shows the variation of $\tilde{\nu}_R$ and γ_R for the symmetric C—H stretch of benzene as it is diluted in benzene- d_6 and in acetone- d_6 . In general the data for benzene are less precise than those for chloroform. The average of the relative standard deviation for the $\tilde{\nu}_R$ measurements is 0.022%. (or $\pm 0.88 \text{ cm}^{-1}$ for this C—H mode), and for the γ_R measurements it is 16.5%. The values of $\tilde{\nu}_R$ and γ_R for neat benzene are $3062.88 \pm 0.61 \text{ cm}^{-1}$ and $0.83 \pm 0.056 \text{ ps}^{-1}$, respectively. The vibrational frequency is seen to blue-shift slightly upon the introduction of benzene- d_6 with $\Delta\tilde{\nu}_R^{(0.5)} = 0.89 \text{ cm}^{-1}$. The frequency blue shift is more pronounced upon dilution with acetone- d_6 ; here

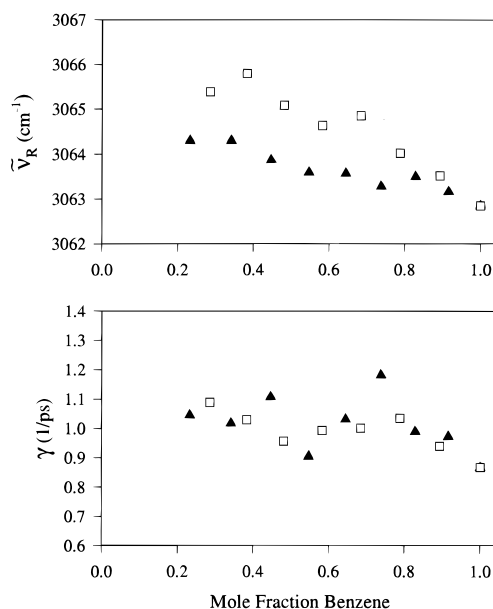


Figure 3. Recovered values of $\tilde{\nu}_R$ and γ for the dilution series of (▲) benzene in benzene- d_6 and (□) benzene in acetone- d_6 .

$\Delta\tilde{\nu}_R^{(0.5)} = 1.87 \text{ cm}^{-1}$. The apparent dephasing rate constant experiences very little change upon dilution with benzene- d_6 and only a slight increase with acetone- d_6 . The value of R_A for neat benzene is found to be 0.245 ± 0.08 . (The results are summarized in Table 1.)

It must be emphasized that in mixtures of intermediate composition “essential” spectral inhomogeneity must exist. The ensemble of resonant two-level systems necessarily encompasses a range of chemically distinct environments. At the very least, any motional line narrowing is under translational diffusional control and cannot reasonably characterize the spectral properties of mixtures. The present treatment (like many others) analyzes the data in mixtures as a single homogeneous line. Thus ω_R represents an apparent central frequency of a distribution of Bohr frequencies, and γ_R represents an average collective dephasing rate constant. For intermediate mole fractions this approach must be regarded as simply empirical. However, a rationalization for simulating the “essential” inhomogeneity by a Lorentzian line has been offered.²⁹ In any case, at the extremes of $X_i = 0, 1$ one often is working with authentic Lorentzian lines.

In measuring absolute frequencies two spectral windows must be calibrated—one containing the narrow-band beam and one containing the I⁽²⁾CARS signal. Interestingly, the broad-band beam need not be finely calibrated. For our setup, such calibration results in an (accuracy) error of $\sim \pm 1 \text{ cm}^{-1}$ on any given absolute frequency measurement. This time—frequency-resolved I⁽²⁾CARS method is particularly well suited for measuring relative frequencies; the large redundancy in the data (up to ~ 1000 -fold) greatly reduces the error of relative measurements. The same redundancy also greatly reduces the error in the γ measurements. For Raman modes that provide a stronger and more slowly decaying I⁽²⁾CARS spectrogram than those seen for these C—H modes, the recovered frequencies (for a given calibration) are extremely reproducible—often having relative standard deviations of $< 0.004\%$ (or 0.04 cm^{-1} for the “ring breathing” modes).²⁹ The typical relative standard deviation for the γ_R measured for these stronger modes remains ~ 5 – 7% like the present chloroform data.

It is, of course, necessary to compare the results obtained by this new method with those from the literature. Previously reported values for $\tilde{\nu}_R$ and γ_R for both benzene and chloroform dilutions series are somewhat varied. For neat chloroform, $\tilde{\nu}_R$

values from¹⁰ 3018 to⁴ 3021 cm⁻¹ have been reported. In one dilution study involving chloroform in carbon tetrachloride,⁴ explicit numbers were not given; we estimate $\Delta\tilde{\nu}_R^{(0.5)} \sim 1.2$ cm⁻¹ in that work (compared to our $\Delta\tilde{\nu}_R^{(0.5)} = 1.67$ cm⁻¹). Our value of 1.03 ps⁻¹ for γ_R of neat chloroform lies between reported values which include^{10,7,4} ~ 0.8 , ~ 0.94 , and ~ 1.13 ps⁻¹. Reference 8 reports an interesting trend in γ_R . A decrease in γ_R is seen upon dilution until roughly 0.4 mole fraction chloroform at which point γ_R then begins to increase. Conversely, in the same system, we see only an essentially monotonic decrease in γ_R (see Figure 3), although there is a slowing of this decrease below ~ 0.5 mole fraction chloroform. In any case, there appears to be good agreement between their $\Delta\gamma_R^{(0.5)}$ (we estimate to be 0.1 ps⁻¹) and our $\Delta\gamma_R^{(0.5)} = 0.10$ ps⁻¹. The temperature difference of 25 °C (ref 4) and 18 °C (this work) is not likely to account for such discrepancies according to temperature studies of γ_R for neat chloroform.¹⁰

For neat benzene, $\tilde{\nu}_R$ values from³⁵ 3061 to¹³ 3063 cm⁻¹ have been reported. Several studies of benzene in benzene-d₆ have been reported.^{5,6,9,13} Our $\Delta\tilde{\nu}_R^{(0.5)} = 0.89$ cm⁻¹ is larger than previous results: $\Delta\tilde{\nu}_R^{(0.5)} = 0.37$ cm⁻¹ (ref 5), $\Delta\tilde{\nu}_R^{(0.5)} = 0.35$ cm⁻¹ (ref 6), and $\Delta\tilde{\nu}_R^{(0.5)} = 0.27$ cm⁻¹ (ref 9). Measures of γ_R for neat benzene include¹³ ~ 0.77 ps⁻¹ and⁸ ~ 0.83 ps⁻¹ (cf. $\gamma_R = 0.85$ ps⁻¹ for this work). Reference 8 reports no change in γ_R upon dilution of benzene with benzene-d₆; we observe a slight increase in γ_R upon dilution. Reference 8 also reports a slight increase in γ_R for dilution with acetone-d₆ as does this work.

IV. Conclusion

We report, for the first time, the down-conversion of the high-frequency symmetric C–H stretch of chloroform and benzene using the time–frequency-resolved I⁽²⁾CARS technique. This method offers the advantages of strong down-conversion of vibrational modes and a near three orders of magnitude redundancy in the data for equal acquisition times and allows (for many systems) highly reliable extraction of dynamic and spectroscopic parameters. It is particularly well suited for relative frequency measurements as well as measurements of absolute dephasing rate constants. However these relatively weak, broad, C–H modes are not optimal in this respect. Dilution studies were performed, and frequency shifts and changes in the dephasing rate constants were obtained and compared to the literature. Chloroform–carbon tetrachloride solutions show a linear red shift of the C–H stretch until approximately 0.5 mole fraction where the rate of the shift begins to decrease upon dilution. The vibrational dephasing rate constant decreases monotonically (but not linearly). Benzene–benzene-d₆ and benzene–acetone-d₆ solutions each shows a blue shift of the C–H stretch upon dilution and an increase in γ , but acetone-d₆ has the greater effect on the frequency shift. Once such data can be regarded as reliable (currently the discrepancy across the literature is unsatisfactory), it will be the task of theory to rationalize such observations. Now we

hope the I⁽²⁾CARS spectrograms may provide a useful way to acquire dependable Raman parameters.

Acknowledgment. We thank R.F. Loring for discussion and directing us to pertinent references. We gratefully acknowledge NSF grant number CHE-9616635. M.J.S. wishes to thank the NIH for support in the form of a biophysical training grant fellowship.

References and Notes

- (1) Oxtoby, D. W. *Adv. Chem. Phys.* **1979**, *40*, 1.
- (2) Morresi, A.; Mariani, L.; Distefano, M. R.; Giorgini, M. G. *J. Raman Spectrosc.* **1995**, *26*, 179.
- (3) Throughout this letter numerical values for vibrational frequencies will be given in wavenumbers: $\tilde{\nu}_R = \omega_R/2\pi c$, where c is the speed of light.
- (4) Fujiyama, T.; Kakimoto, M.; Suzuki, T. *Bull. Chem. Soc. Jpn.* **1976**, *49*, 606.
- (5) Kamogawa, K.; Kitagawa, T. *J. Phys. Chem.* **1990**, *94*, 3916.
- (6) Laane, J.; Kiefer, W. *Appl. Spectrosc.* **1981**, *35*, 428.
- (7) Laane, J.; Kiefer, W. *J. Chem. Phys.* **1980**, *73*, 4971.
- (8) Tanabe, K.; Jonas, J. *Chem. Phys. Lett.* **1978**, *53*, 278.
- (9) Meinanader, N.; Strube, M. M.; Johnson, A. N.; Laane, J. *J. Chem. Phys.* **1987**, *86*, 4762.
- (10) Fukuda, T.; Ikawa, S.; Kimura, M. *Chem. Phys.* **1989**, *133*, 151.
- (11) Benson, A. M., Jr.; Drickamer, H. G. *J. Chem. Phys.* **1957**, *27*, 1164.
- (12) Fukushi, K.; Fukada, T.; Kimura, M. *J. Raman Spectrosc.* **1987**, *18*, 47.
- (13) Seifert, F.; Oehme, K.-L.; Rudakoff, G.; Hölzer, W.; Carius, W.; Schröter, O. *Chem. Phys. Lett.* **1984**, *105*, 636.
- (14) Nomura, H.; Koda, S.; Miyahara, Y. *Bull. Chem. Soc. Jpn.* **1979**, *52*, 3249.
- (15) Tananbe, K.; Jonas, J. *J. Chem. Phys.* **1977**, *67*, 4222.
- (16) Schroeder, J.; Schiemann, V. H.; Jonas, J. *J. Chem. Phys.* **1978**, *69*, 5479.
- (17) Morita, N.; Yajima, T. *Phys. Rev. A* **1984**, *30*, 2525.
- (18) Kobayashi, T. *Adv. Chem. Phys.* **1994**, *85*, 55.
- (19) Kummrow, A.; Lau, A. *Appl. Phys. B* **1996**, *63*, 209.
- (20) Albrecht, A. C.; et al. *Laser Phys.* **1995**, *5*, 667.
- (21) The I stands for interferometric—a central feature of all noisy light spectroscopies. The superscript (2) denotes the fact that two noisy fields act in the development of the induced polarization that is responsible for the signal.
- (22) Dugan, M. A.; Mellinger, J. S.; Albrecht, A. C. *Chem. Phys. Lett.* **1988**, *147*, 411.
- (23) Dugan, M. A.; Albrecht, A. C. *Phys. Rev. A* **1991**, *43*, 3877.
- (24) Dugan, M. A.; Albrecht, A. C. *Phys. Rev. A* **1991**, *43*, 3922.
- (25) Schaertel, S. A.; Albrecht, A. C.; Lau, A.; Kummrow, A. *Appl. Phys. B* **1994**, *59*, 377.
- (26) Schaertel, S. A.; Albrecht, A. C. *J. Raman Spectrosc.* **1994**, *25*, 545.
- (27) In earlier references^{20–26} these oscillations were referred to as Rabi detuning oscillations.
- (28) Stimson, M. J.; Ulness, D. J.; Albrecht, A. C. *Chem. Phys. Lett.* **1996**, *263*, 185.
- (29) Stimson, M. J.; Ulness, D. J.; Albrecht, A. C. Submitted to *Chem. Phys.*
- (30) Mukamel, S. *Principles of Nonlinear Optical Spectroscopy*; Oxford University Press: New York, 1995.
- (31) The exact equation for the I⁽²⁾CARS signal is given in refs 25 and 26.
- (32) Shirley, J. A.; Hall, R. J.; Eckbreth, A. C. *Opt. Lett.* **1980**, *5*, 380.
- (33) Press, W. H.; Flannery, B. P.; Teukolsky, S. A.; Vetterling, W. T. *Numerical Recipes in C*; Cambridge University Press: New York, 1988.
- (34) Ulness, D. J.; Stimson, M. J.; Kirkwood, J. C.; Albrecht, A. C. Submitted to *J. Raman Spectrosc.*
- (35) Gruhl, H.; Periasamy, N. *Chem. Phys. Lett.* **1983**, *95*, 352.